

Teleportation of atomic states via position measurements

Michele Tumminello^{1,2} and Francesco Ciccarello^{3,1}

¹*Dipartimento di Fisica e Tecnologie Relative, Università di Palermo, Viale delle Scienze, I-90128 Palermo, Italy*

²*CNR-INFM, Unità di Palermo, Palermo, Italy**

³*NEST and Dipartimento di Scienze Fisiche ed Astronomiche, Università di Palermo, Via Archirafi 36, I-90123 Palermo, Italy*

We present a scheme for conditionally teleporting an unknown atomic state in cavity QED which requires two atoms and one cavity mode. The translational degrees of freedom of the atoms are taken into account using the optical Stern-Gerlach model. We show that successful teleportation with probability 1/2 can be achieved through local measurements of the cavity photon number and atomic positions. Neither Bell-state measurement nor holonomous interaction-time constraints are required.

PACS numbers: 42.50.-p, 32.80.Lg, 03.65.Ud

I. INTRODUCTION

Quantum entanglement, maybe the most intriguing feature of quantum mechanics [1], is a powerful resource for quantum information processing tasks [2].

An outstanding application of entanglement is the teleportation of an unknown qubit, the unit of quantum information, between two systems. In the seminal paper by Bennett *et al.* [3], a quantum state is transferred from qubit *A* to qubit *B* using an *ancilla*, e.g. a third auxiliary qubit *C*. Qubits *B* and *C* are initially prepared in an entangled state. A Bell measurement on *A* and *C* is then made. Depending on the outcome of such measurement, a suitable unitary transformation on *B* is performed in order to reconstruct the initial quantum state of *A*. Teleportation is successful with probability 1/4. Soon after the proposal by Bennett *et al.*, quantum teleportation has received considerable attention culminated in its experimental demonstration in a number of works [4, 5, 6, 7].

Cavity QED systems – where Rydberg atoms couple to the quantized electromagnetic (e.m.) field of a superconductive cavity [8] – have received considerable attention during the last years [9]. Cavity QED systems have been proposed for implementing teleportation protocols of internal quantum states between atoms, a task which is particularly attractive especially after its experimental proof for trapped ion systems [10]. Generally speaking, in such cavity QED schemes a quantum internal state is teleported between two atoms via coherent interaction with cavity field modes and/or auxiliary atoms which act as quantum channels.

Quite recently, efforts have been made for achieving teleportation without any Bell-state measurement [11, 12, 13, 14, 15]. In particular, Zheng has proposed a scheme for approximately teleporting an unknown internal state between two atoms which successively interact

with a cavity mode according to the Jaynes-Cummings Hamiltonian [13]. The probability of success is 1/4 and no Bell-State measurement is required. Ye and Guo have presented another no Bell-state measurement scheme which makes use of three atoms and a single-mode cavity field out of resonance [14]. The atom-atom coupling via the virtual excitations of the cavity field is exploited for teleporting a quantum state between two atoms with probability of success 1/2. Both the above schemes require precise tuning of the atom-cavity field interaction time.

To our knowledge, no cavity QED-teleportation scheme has so far accounted for the translational dynamics of atoms flying through a cavity. Indeed, the spatial structure of the quantum e.m. field along the *x*-cavity axis affects the internal dynamics of a flying atom. This leads to an atom-field coupling constant which in fact depends on the atomic translational degrees of freedom along the *x*-direction. Such circumstance – taking place whenever the atomic wavepacket has a width non negligible with respect to the field wavelength – has been shown to give rise to a number of observable phenomena such as optical Stern-Gerlach effect [16], self-induced transparency [17], modulation of the atomic decay in a damped cavity [18], non-dissipative damping of the Rabi oscillations [19, 20].

It is clear that the involvement of the translational degrees of freedom introduces non-dissipative decoherence in the atom-field dynamics. Such effect, stemming from the entanglement between the atom-field system and the atomic translational degrees of freedom, has been shown to spoil the non-local correlations between two atoms which successively interact with the same cavity mode [21, 22]. Accordingly, the inclusion of the translational dynamics is thus expected to decrease the efficiency of those teleportation protocols relying on the coherent atom-cavity mode coupling.

However, a different perspective can be adopted. Indeed, one may wonder whether such additional degrees of freedom could be fruitfully exploited as a resource for attaining efficient atomic teleportation provided that measurements of the atomic positions are performed. Ac-

*Electronic address: tumminello@lagash.dft.unipa.it

ording to such a scenario, the atomic translational degrees of freedom play the role of further quantum channels able to transfer information between the internal degrees of freedom of different atoms.

A crucial motivation in the search for such a teleportation protocol is that, according to the optical Stern-Gerlach model, the wavefunction of a two-level atom entering a cavity generally splits into a set of deflected wavepackets, each corresponding to a different atom-field dressed state [19, 23]. For an increasing atom-cavity interaction time, such outgoing wavepackets become more and more distinguishable up to the point that *which-path* information becomes accessible [20]. This information is used in our protocol for attaining conditional transfer of quantum information between two atoms which successively interact with the same cavity mode. This is indeed the central mechanism underlying the physics presented in this work.

In this paper, we consider two atoms which successively enter the same cavity in either a nodal or antinodal region of the corresponding field mode. Each atom interacts with such mode according to the optical Stern-Gerlach Hamiltonian. This can be approximated as a linear (quadratic) expansion in the atomic position along the cavity axis when a nodal (antinodal) region is considered. Both the atoms are assumed to enter the cavity in a given minimum uncertainty Gaussian wave packet with the target atom and the resonant mode initially in the excited and vacuum state, respectively. We show that conditional teleportation of an internal atomic state can be achieved by local measurements of the atomic positions, the cavity photon-number and the internal state of the atom whose state is to be transmitted. No Bell-state measurement is required. We thus prevent the projection of our two-atoms system onto highly entangled subspaces, therefore avoiding the need of (in general quite difficult) joint measurements. This is a major advantage of no Bell-state measurement teleportation schemes. Furthermore, at variance with other cavity-QED protocols which work without Bell-state measurement [13, 14], no holonomous constraints on the atom-cavity interaction times are required. It only suffices that the time of flight of each atom inside the cavity is long enough in order for the outgoing deflected wavepackets to be distinguished with reasonable approximation. We show that successful teleportation of an atomic state can be attained with probability 1/2.

This paper is organized as follows. In Sec. II, we introduce the system and the Hamiltonian both in the nodal and in the antinodal case. In Sec. III, the main part of this work, we describe the teleportation scheme. A relevant property the protocol relies on is the *which-path* information about the outgoing atomic wave packets. The conditions allowing this information to be accessible are reviewed and discussed in Sec. IV. Finally, in Sec. V, we draw our conclusions.

II. SYSTEM AND APPROACH

We consider two identical two-level atoms, labeled 1 and 2, of mass m and Bohr frequency ω . The atoms interact in succession with the e.m. field of the same e.m. cavity. We assume that the velocity of each atom along the z -direction (orthogonal to the x -cavity axis) is large enough that the motion along the z -axis can be treated classically. Denoting by a and a^\dagger the annihilation and creation operators of the cavity field and assuming the resonance condition, the free Hamiltonian H_0 can be written as

$$H_0 = \sum_{i=1,2} \left[\frac{\hat{p}_i^2}{2m} + \hbar\omega S_{z,i} \right] + \hbar\omega a^\dagger a, \quad (1)$$

where – for each atom $i = 1, 2$ – $S_{z,i}, S_{\pm,i}$ are the usual spin-1/2 operators and $\hat{p}_i = -i\hbar(d/dx_i)$ is the x -component of the momentum operator. In the Rotating Wave Approximation, each atom i couples to the cavity field according to the interaction Hamiltonian

$$H_i = \hbar\varepsilon \sin(k\hat{x}_i) (a^\dagger S_{-,i} + a S_{+,i}) \quad (i = 1, 2) \quad (2)$$

with k and ε standing for the wave number of the e.m. mode and the atom-field coupling constant, respectively, and where \hat{x}_i is the i th atomic position operator along the cavity axis.

When both the atoms enter the cavity in a nodal region of the cavity mode with the width σ_{x_i} of their respective wavepackets small enough compared to $2\pi/k$ ($\sigma_{x_i} \ll 2\pi/k$), H_i can be approximated as a linear expansion in the atomic position

$$H_{iN} = \hbar\varepsilon k \hat{x}_i (a^\dagger S_{-,i} + a S_{+,i}), \quad (3)$$

while in an antinodal region it takes the form

$$H_{iA} = \hbar\varepsilon \left(1 - \frac{k^2 \hat{x}_i^2}{2} \right) (a^\dagger S_{-,i} + a S_{+,i}). \quad (4)$$

In Eqs. (3) and (4), \hat{x}_i stands for the atomic position operator of the i th atom with respect to a nodal point and an antinodal point, respectively.

At time $t = 0$, atom 1 enters the cavity and interacts with the field for a time t_1 . At a later time $t_2 > t_1$, atom 2 enters the cavity and couples to the field state modified by the first atom. At time $t_3 > t_2$ atom 2 exits the cavity. At times $t \geq t_3$ both the atoms are therefore out of the cavity and evolve freely. In the interaction picture, the Hamiltonian at all times, respectively in a nodal and antinodal region of the cavity field, reads

$$H_N^I(t) = \hbar\varepsilon k \left(\hat{x}_1 + \frac{\hat{p}_1}{m} t \right) \mu_1(0, t_1) u_1 + \hbar\varepsilon k \left(\hat{x}_2 + \frac{\hat{p}_2}{m} t \right) \mu_2(t_2, t_3) u_2, \quad (5)$$

where we have introduced the atom-field operators $u_i = a^\dagger S_{-,i} + a S_{+,i}$ and where the time interval during which

each atom interacts with the cavity mode is accounted for through the function $\mu_t(t', t'') = \theta(t - t') - \theta(t - t'')$, $\theta(t)$ being the usual Heaviside function.

In an antinodal region of the cavity field, the Hamiltonian in the interaction picture takes the form

$$H_A^I(t) = \hbar\varepsilon \left[1 - \frac{k^2}{2} \left(\hat{x}_1 + \frac{\hat{p}_1}{m}t \right)^2 \right] \mu_t(0, t_1) u_1 \\ + \hbar\varepsilon \left[1 - \frac{k^2}{2} \left(\hat{x}_2 + \frac{\hat{p}_2}{m}t \right)^2 \right] \mu_t(t_2, t_3) u_2. \quad (6)$$

Of course, in the time interval $[t_1, t_2]$ and for $t \geq t_3$ both $H_N^I(t)$ and $H_A^I(t)$ vanish since no atom is inside the cavity. The Hamiltonian operators of Eqs. (5) and (6) can be used to derive the exact dynamics of a given initial state of the two-atom-field system at times $t \geq t_3$. This is accomplished through the respective evolution operators $U_\alpha^I(t \geq t_3)$

$$U_\alpha^I(t \geq t_3) = T \exp \left[-\frac{i}{\hbar} \int_0^{t_3} H_\alpha^I(t) dt \right] \quad (\alpha = N, A) \quad (7)$$

with T standing for the time-ordering operator and where the second integration bound is due to the fact that $H_\alpha^I = 0$ for $t \geq t_3$.

Due to the fact that atom 2 enters the cavity after atom 1 has come out of it, it is possible to split up $U_\alpha^I(t \geq t_3)$ into the product of two evolution operators $U_{\alpha,1}^I(t \geq t_3)$ and $U_{\alpha,2}^I(t \geq t_3)$ ($\alpha = N, A$). Each operator $U_{\alpha,i}^I(t \geq t_3)$ only affects the dynamics of atom i . In formulae (from now on, whenever unnecessary, the time argument “ $t \geq t_3$ ”) and/or the apex “ I ” in the evolution operators will be omitted)

$$U_\alpha = U_{\alpha,2} \cdot U_{\alpha,1} \quad (\alpha = N, A) \quad (8)$$

with

$$U_{\alpha,1} = T \exp \left[-\frac{i}{\hbar} \int_0^{t_1} H_\alpha^I(t) dt \right] = U_{\alpha,1}(\hat{x}_1, \hat{p}_1, u_1), \quad (9)$$

$$U_{\alpha,2} = T \exp \left[-\frac{i}{\hbar} \int_{t_2}^{t_3} H_\alpha^I(t) dt \right] = U_{\alpha,2}(\hat{x}_2, \hat{p}_2, u_2), \quad (10)$$

where in the right-hand side of both equations we have explicitly indicated the operators each $U_{\alpha,i}$ depends on according to Eqs. (5) and (6).

III. TELEPORTATION SCHEME

We denote the ground and excited states of the i th atom by $|g_i\rangle$ and $|e_i\rangle$, respectively. Assume that atom 2 is the one whose initial internal state, say $|\alpha_2\rangle$, is to be teleported. Such state is written as

$$|\alpha_2\rangle = \cos \frac{\vartheta}{2} |e_2\rangle + e^{i\varphi} \sin \frac{\vartheta}{2} |g_2\rangle \quad (11)$$

with $\vartheta \in [0, \pi]$ and $\varphi \in [0, \pi]$.

By indicating the Fock states of the cavity field as $|n\rangle$ ($n = 0, 1, \dots$), we consider the following initial state of the system:

$$|\Psi(0)\rangle = |\varphi_1(0)\rangle |e_1\rangle |\varphi_2(0)\rangle |\alpha_2\rangle |0\rangle, \quad (12)$$

where $|\varphi_i(0)\rangle$ (associated with each atom $i = 1, 2$) is a Gaussian wavepacket of minimum uncertainty, such that the product between the initial position and momentum widths fulfills $\sigma_{x_i} \cdot \sigma_{p_i} = \hbar/2$.

Consider now the usual dressed states of the i th atom $|\chi_{n,i}^\pm\rangle = (|e_i\rangle |n\rangle \pm |g_i\rangle |n+1\rangle) / \sqrt{2}$ ($n = 0, 1, \dots$). These states are eigenstates of the u_i operators since $u_i |\chi_{n,i}^\pm\rangle = \pm \sqrt{n+1} |\chi_{n,i}^\pm\rangle$ (while $u_i |g_i\rangle |0\rangle = 0$). The dressed states together with $|g_i\rangle |0\rangle$ ($i = 1, 2$) represent an orthonormal basis of the corresponding Hilbert space. It is important to notice that u_i commutes with $U_{\alpha,i}$ according to Eqs. (9) and (10) and the corresponding Hamiltonian operators of Eqs. (5) and (6). It follows that the effective representation $U_{\alpha,i}^{(n,\pm)}$ of $U_{\alpha,i}$, as applied to a dressed state $|\chi_{n,i}^\pm\rangle$, is obtained by simply replacing u_i with $\pm \sqrt{n+1}$ in Eqs. (9) and (10). This yields

$$U_{\alpha,i}^{(n,\pm)} = U_{\alpha,i}(\hat{x}_i, \hat{p}_i, \pm \sqrt{n+1}) \quad (n = 0, 1, \dots), \quad (13)$$

while the effective representation of $U_{N,i}$ – as applied to state $|g_i\rangle |0\rangle$ – reduces to the identity operator for both the atoms $i = 1, 2$.

The operators in Eq.(13) clearly affect only the atomic translational dynamics and therefore allow to define a family of atomic translational wavepackets $|\Phi_{\alpha,n,i}^\pm\rangle$ according to

$$|\Phi_{\alpha,n,i}^\pm\rangle = U_{\alpha,i}^{(n,\pm)} |\varphi_i(0)\rangle, \quad (14)$$

such that

$$U_{\alpha,i} |\varphi_i(0)\rangle |\chi_{n,i}^\pm\rangle = |\Phi_{\alpha,n,i}^\pm\rangle |\chi_{n,i}^\pm\rangle. \quad (15)$$

Once the time evolution operator (8) is applied to $|\Psi(0)\rangle$, the state of the whole system at a time $t \geq t_3$ – when both the atoms are out of the cavity – can be written in the form (from now on, the index α in the Φ states will be omitted)

$$|\psi(t_3)\rangle = |\lambda_{0,1}\rangle |\varphi_2(0)\rangle |g_2\rangle |0\rangle \\ + \sum_{n=0,1} \sum_{\eta=-,+} (|\lambda_{n,1}^\eta\rangle |\Phi_{n,2}^\eta\rangle |\chi_{n,2}^\eta\rangle), \quad (16)$$

where the λ states of atom 1 are defined according to

$$|\lambda_{0,1}\rangle = \left(\frac{|\Phi_{0,1}^+\rangle + |\Phi_{0,1}^-\rangle}{2} \right) e^{i\varphi} \sin \frac{\vartheta}{2} |e_1\rangle, \quad (17)$$

$$|\lambda_{0,1}^\pm\rangle = \left(\frac{|\Phi_{0,1}^+\rangle + |\Phi_{0,1}^-\rangle}{2\sqrt{2}} \right) \cos \frac{\vartheta}{2} |e_1\rangle \\ \pm \left(\frac{|\Phi_{0,1}^+\rangle - |\Phi_{0,1}^-\rangle}{2\sqrt{2}} \right) e^{i\varphi} \sin \frac{\vartheta}{2} |g_1\rangle, \quad (18)$$

$$|\lambda_{1,1}^\pm\rangle = \left(\frac{|\Phi_{0,1}^+\rangle - |\Phi_{0,1}^-\rangle}{2\sqrt{2}} \right) \cos \frac{\vartheta}{2} |g_1\rangle. \quad (19)$$

The procedure for obtaining state $|\psi(t_3)\rangle$ is detailed in Appendix A. In what follows, we shall indicate the time spent inside the cavity by atoms 1 and 2 with $\tau_1 = t_2 - t_1$ and $\tau_2 = t_3 - t_2$ respectively. The states $|\Phi_{n,i}^\pm\rangle$ appearing in Eq. (16) fulfill the following important property both in the nodal and antinodal case [20, 21, 22]

$$\lim_{\tau_i \rightarrow \infty} \langle \Phi_{n,i}^+ | \Phi_{n,i}^- \rangle = 0. \quad (20)$$

Such property, together with the features of the outgoing

wavepackets $|\Phi_{n,i}^+\rangle$, is discussed in Sec. IV.

According to Eq. (20), wavepackets $|\Phi_{n,i}^+\rangle$ and $|\Phi_{n,i}^-\rangle$ exhibit a negligible overlap for long enough times of flight τ_i . As shown in Refs. [21, 22], times of flight of the order of a few Rabi oscillations are sufficient in order to get negligible overlapping [24].

Such outstanding circumstance makes it possible to distinguish the elements of the set of translational states $\{|\Phi_{n,i}^\pm\rangle\}$ through measurements of the atomic positions along the x -axis [25].

It is straightforward to show that Eq. (20) implies that all the terms appearing in (16) are orthogonal provided that τ_1 and τ_2 are sufficiently large.

Once the dressed states $|\chi_{n,2}^\pm\rangle$ appearing in Eq. (16) are rewritten in terms of states $|g_2\rangle|n\rangle$ and $|e_2\rangle|n\rangle$, one recognizes the occurrence of cases where measurements of the photon number, of the internal state of atom 2 and of the positions of the two atoms can make atom 1 collapse into the initial internal state of atom 2 [Eq.(11)]. Namely a successful teleportation can take place. For instance, the projection of $|\psi(t_3)\rangle$ onto the the cavity field state $|1\rangle$ gives

$$\langle 1 | \psi(t_3) \rangle = \left[\frac{(|\Phi_{0,1}^+\rangle + |\Phi_{0,1}^-\rangle)(|\Phi_{0,2}^+ - \Phi_{0,2}^-)}{4} \cos \frac{\vartheta}{2} |e_1\rangle + \frac{(|\Phi_{0,1}^+ - \Phi_{0,1}^-)(|\Phi_{0,2}^+ + \Phi_{0,2}^-)}{4} e^{i\varphi} \sin \frac{\vartheta}{2} |g_1\rangle \right] |g_2\rangle \\ + \left[\frac{(|\Phi_{0,1}^+ - \Phi_{0,1}^-)(|\Phi_{1,2}^+ + \Phi_{1,2}^-)}{4} \cos \frac{\vartheta}{2} |g_1\rangle \right] |e_2\rangle. \quad (21)$$

This outcome occurs with probability $(3 + \cos \vartheta)/8$. Assume now that a further measurement of the internal state of atom 2 is made. If the outcome of such measurement is $|e_2\rangle$, atom 1 is projected onto the ground state $|g_1\rangle$ and thus no teleportation of the initial state of atom 2 has occurred. The unconditional probability for this event is calculated to be $(1 + \cos \vartheta)/8$.

However, it can be noticed that if atom 2 is found in the ground state $|g_2\rangle$ a further measurement of the atomic positions with outcomes $|\Phi_{0,1}^+\rangle|\Phi_{0,2}^+\rangle$ or $|\Phi_{0,1}^-\rangle|\Phi_{0,2}^-\rangle$ projects atom 1 into the state $|\alpha_1\rangle = \cos \frac{\vartheta}{2} |e_1\rangle + e^{i\varphi} \sin \frac{\vartheta}{2} |g_1\rangle$. This means that state $|\alpha_2\rangle$ of Eq. (11) has been in fact teleported into atom 1.

On the other hand, when the wavepackets $|\Phi_{0,1}^+\rangle|\Phi_{0,2}^-\rangle$ or $|\Phi_{0,1}^-\rangle|\Phi_{0,2}^+\rangle$ are found (after that the state $|g_2\rangle$ has been measured) atom 1 collapses into the state

$$|\alpha_1'\rangle = \cos \frac{\vartheta}{2} |e_1\rangle - e^{i\varphi} \sin \frac{\vartheta}{2} |g_1\rangle, \quad (22)$$

which can be easily transformed into (11) through a 180 degree rotation around the z -axis in order to faithfully

reproduce the initial state of atom 2 and complete the teleportation. Of course, rigorously speaking, the measurements of the atomic positions do not formally correspond to projections onto states $|\Phi_{0,i}^+\rangle$ and $|\Phi_{0,i}^-\rangle$. However, due to the discussed orthogonality of $|\Phi_{0,i}^+\rangle$ and $|\Phi_{0,i}^-\rangle$, such translational states can be associated with different atomic paths l_i^+ and l_i^- . The measurements of the atomic positions cause indeed effective projections on such paths.

Note that the above teleportation scheme, conditioned to the outcome $|g_2\rangle|1\rangle$, is invariant for a change of each l_i^+ into l_i^- and vice-versa. This implies that for each atom $i = 1, 2$ the labeling of the two paths is arbitrary. If both the atoms are found in a path “+” or in a path “-”, atom 1 is projected into state (11). If the paths of the two atoms have different signs, regardless of which atom is in which path, state (22) is obtained and the teleportation process can be finalized once a 180 degree rotation on the internal state of atom 1 is applied.

In a similar way, it turns out that, when the field vacuum state $|0\rangle$ is found, the outcome $|g_2\rangle$ cannot transfer

Photons	Atom 2	Path atom 1	Path atom 2	Teleportation	Internal state atom 1	Failure probability
2	–	–	–	Unsuccessful	–	$\frac{1}{8}(1 + \cos \vartheta)$
1	$ e_2\rangle$	–	–	Unsuccessful	–	$\frac{1}{8}(1 + \cos \vartheta)$
	$ g_2\rangle$	l_1^-	l_2^-	Successful	$\cos \frac{\vartheta}{2} e_1\rangle + e^{i\varphi} \sin \frac{\vartheta}{2} g_1\rangle$	–
	$ g_2\rangle$	l_1^-	l_2^+	Successful [26]	$\cos \frac{\vartheta}{2} e_1\rangle - e^{i\varphi} \sin \frac{\vartheta}{2} g_1\rangle$	–
	$ g_2\rangle$	l_1^+	l_2^+	Successful	$\cos \frac{\vartheta}{2} e_1\rangle + e^{i\varphi} \sin \frac{\vartheta}{2} g_1\rangle$	–
	$ g_2\rangle$	l_1^+	l_2^-	Successful [26]	$\cos \frac{\vartheta}{2} e_1\rangle - e^{i\varphi} \sin \frac{\vartheta}{2} g_1\rangle$	–
0	$ g_2\rangle$	–	–	Unsuccessful	–	$\frac{1}{4}(1 - \cos \vartheta)$
	$ e_2\rangle$	l_1^-	l_2^-	Successful	$\cos \frac{\vartheta}{2} e_1\rangle + e^{i\varphi} \sin \frac{\vartheta}{2} g_1\rangle$	–
	$ e_2\rangle$	l_1^-	l_2^+	Successful [26]	$\cos \frac{\vartheta}{2} e_1\rangle - e^{i\varphi} \sin \frac{\vartheta}{2} g_1\rangle$	–
	$ e_2\rangle$	l_1^+	l_2^+	Successful	$\cos \frac{\vartheta}{2} e_1\rangle + e^{i\varphi} \sin \frac{\vartheta}{2} g_1\rangle$	–
	$ e_2\rangle$	l_1^+	l_2^-	Successful [26]	$\cos \frac{\vartheta}{2} e_1\rangle - e^{i\varphi} \sin \frac{\vartheta}{2} g_1\rangle$	–

TABLE I: Teleportation measurement scheme. Each case is represented by given outcomes of the number of photons (1st column), the internal state of atom 2 (2nd column), and the paths along which the two atoms are found (3th and 4th columns). In the 5th column it is indicated whether or not teleportation has been successful. If successful, the state onto which atom 1 is projected ($|\alpha_1\rangle$ or $|\alpha'_1\rangle$) is presented (6th column). If unsuccessful, the associated unconditional failure probability is given in the last column.

the initial state of atom 2 into atom 1, while successful teleportation is attained when atom 2 is found to be in the excited state $|e_2\rangle$. As in the case $|g_2\rangle|1\rangle$, when the atoms are found in the same quantum path (i.e. l_1^+ and l_2^+ or l_1^- and l_2^-) the first atom is projected into $|\alpha_1\rangle$. Again, when different quantum paths are found (i.e. l_1^+ and l_2^- or l_1^- and l_2^+) teleportation can be finalized after a 180 degree rotation around the z -axis. Due to conservation of $\sum_{i=1,2} S_{z,i} + a^\dagger a$, no teleportation is possible when the field is found to be in $|2\rangle$.

All the possible events are summarized in Table I. For

each case – corresponding to given outcomes of the number of photons (1st column), the internal state of atom 2 (2nd column), and the paths along which the two atoms are found (3th and 4th columns) – it is shown whether or not teleportation has been successful or not (5th column). If successful, the state onto which atom 1 is projected ($|\alpha_1\rangle$ or $|\alpha'_1\rangle$) is presented (6th column). If unsuccessful, the associated unconditional failure probability is given (last column). A schematic diagram of the teleportation protocol is presented in Fig. 1.

The total failure probability, obtained as the sum of the unconditioned failure probabilities (last column of Table I), is 1/2. Teleportation is thus successful with probability 1/2.

Furthermore, no Bell-state measurement is required in our scheme since teleportation can be finalized through local operations on the two atoms and the cavity field.

Finally, unlike previous no Bell-state measurement-cavity QED protocols [13, 14], the interaction time of each atom with the cavity does not need to fulfill any holonomous constraint. It is only required that it is large enough in order for (20) to hold with reasonable approximation.

IV. ORTHOGONALITY OF THE OUTGOING ATOMIC WAVEPACKETS AND WHICH-PATH INFORMATION

In this section, we discuss in more details the features of the translational states introduced in Eq. (14) and the conditions for *which path* information to be accessible.

In the nodal case, using Eqs. (5), (9), (10) and (14), the outgoing translational wavepackets $|\Phi_{n,i}^\pm\rangle$ take the form

$$\begin{aligned}
|\Phi_{n,1}^\pm\rangle &= U_{N,1}^{(n,\pm)} |\varphi_1(0)\rangle = \\
&= \exp[i\hbar \frac{\varepsilon^2 k^2}{12m} (n+1)t_1^3] \\
&\quad \cdot \exp[\mp i\varepsilon k \sqrt{n+1}t_1 (\hat{x}_1 + \frac{\hat{p}_1}{2m}t_1)] |\varphi_1(0)\rangle,
\end{aligned} \tag{23}$$

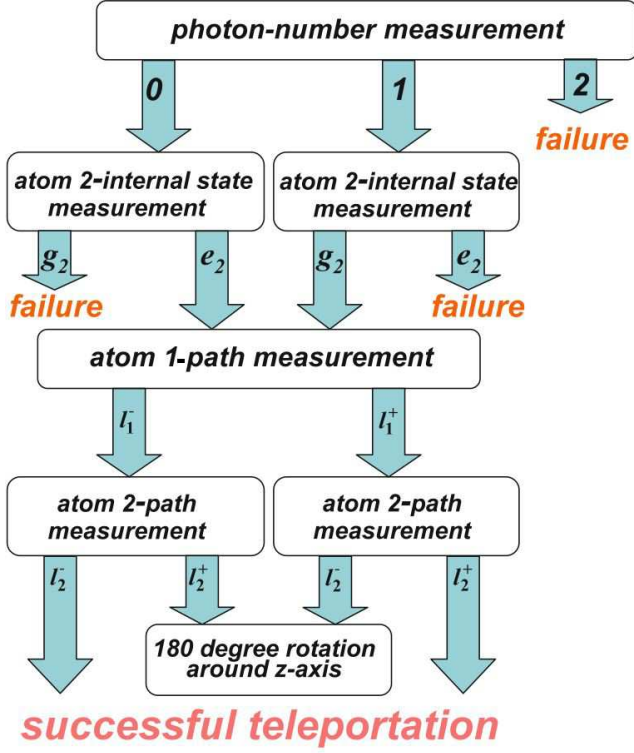


FIG. 1: (Color online) Schematic diagram of the teleportation protocol.

and

$$\begin{aligned}
 |\Phi_{n,2}^{\pm}\rangle &= U_{N,2}^{(n,\pm)} |\varphi_2(0)\rangle = \\
 &= \exp\{\mp i\varepsilon k\sqrt{n+1}(t_3 - t_2)[\hat{x}_2 + \frac{\hat{p}_2}{2m}(t_3 + t_2)]\} \\
 &\cdot \exp[i\hbar\frac{\varepsilon^2 k^2}{12m}(n+1)(t_3 - t_2)^3] |\varphi_2(0)\rangle. \quad (24)
 \end{aligned}$$

Using Eqs. (23) and (24), it can be shown that [19, 20, 21]

$$\begin{aligned}
 \langle\Phi_{n,i}^+|\Phi_{n,i}^-\rangle(\tau_i) &= \exp[-i(2\varepsilon k\sqrt{n+1}x_{0,i})\tau_i] \cdot \\
 &\cdot \exp\left[-(n+1)\left(\frac{\hbar\varepsilon k}{m}\right)\left(\frac{\tau_i^2}{8\sigma_{x_i}^2} + \frac{4m^2}{8\sigma_{p_i}^2}\right)\tau_i^2\right], \quad (25)
 \end{aligned}$$

where $x_{0,i}$ stands for the initial average value of the atomic position along the cavity axis. Eq. (25) clearly shows the presence of a damping factor which causes the scalar products $\langle\Phi_{n,i}^+|\Phi_{n,i}^-\rangle$ to vanish at long times. This proves Eq. (20) in the nodal case.

Such behavior, which is at the origin of the non-dissipative damping of the Rabi oscillations [19, 20], arises from the increasing distance in the phase space [27] of the deflected outgoing components $|\Phi_{n,i}^{\pm}\rangle$ of the incoming wavepacket $|\varphi_i(0)\rangle$ [28]. To better highlight this phenomenon, Eq.(25) can indeed be rewritten in the form [19] (from now on, the subscript i will be omitted

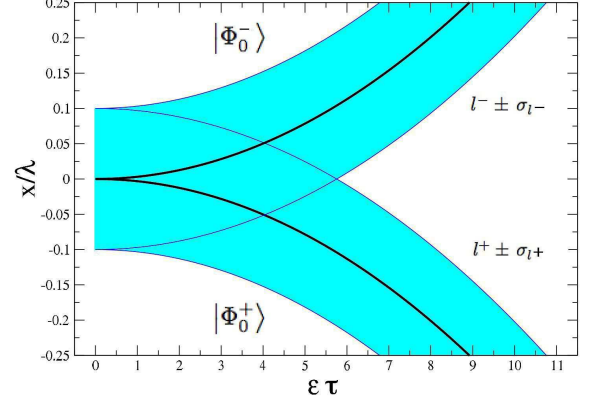


FIG. 2: Quantum paths $l^{\pm} \pm \sigma_{l\pm}$ and $l^{\mp} \pm \sigma_{l\mp}$, associated with wavepackets $|\Phi_0^{\pm}\rangle$, versus the rescaled atom-cavity interaction time $\varepsilon\tau$. The parameters used are: $\lambda = 10^{-5}\text{m}$, $\varepsilon = 10^5 \text{sec}^{-1}$, $m = 10^{-26} \text{kg}$, $\sigma_x = \lambda/10$ and $x_0 = p_0 = 0$.

for simplicity)

$$\begin{aligned}
 \langle\Phi_n^+|\Phi_n^-\rangle(\tau) &= e^{-i\Omega_n(\tau)\tau} \exp\left\{-\frac{[x_n^+(\tau) - x_n^-(\tau)]^2}{8\sigma_x^2} \right. \\
 &\quad \left. - \frac{[p_n^+(\tau) - p_n^-(\tau)]^2}{8\sigma_p^2}\right\} \quad (26)
 \end{aligned}$$

with

$$\Omega_n(\tau) = 2k\varepsilon\sqrt{n+1}\left(x_0 + \frac{p_0}{2m}\tau\right), \quad (27)$$

$$x_n^{\pm}(\tau) = x_0 + \frac{p_0}{m}\tau \mp \frac{\hbar k\varepsilon}{2m}\sqrt{n+1}\tau^2, \quad (28)$$

$$p_n^{\pm}(\tau) = p_0 \mp \hbar k\varepsilon\sqrt{n+1}\tau. \quad (29)$$

Here p_0 stands for the initial average momentum. The above equations show that wavepackets $|\Phi_n^+\rangle$ and $|\Phi_n^-\rangle$ respectively represent negatively and positively deflected components of the input wavepacket, the deflection getting larger as n and/or the atom-cavity interaction time τ grow. This is the reason why, when the interaction time of each atom with the cavity is large enough, *which-path* information becomes accessible so that the quantum paths associated with states $|\Phi_n^{\pm}\rangle$ can be distinguished (see Sec. III). In order to better illustrate such effect, we consider an atom of mass $m = 10^{-26} \text{kg}$ entering the cavity in a nodal region. Assume that the initial translational state of the atom is a Gaussian wavepacket of width $\sigma_x = \lambda/10$ ($\lambda = 2\pi/k = 10^{-5}\text{m}$) with $x_0 = p_0 = 0$ and that the atom-field coupling constant $\varepsilon = 10^5 \text{sec}^{-1}$. The resulting quantum paths l^{\pm} associated with wavepackets $|\Phi_0^{\pm}\rangle$ (i.e. those involved in the teleportation scheme) are shown in Fig. 1 together with their widths $\sigma_{l\pm}$ (i.e. the standard deviations of

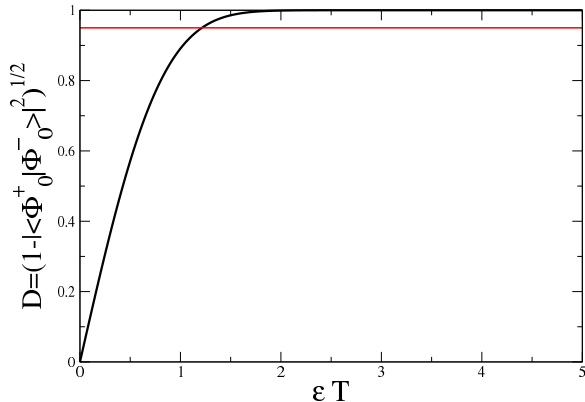


FIG. 3: Distinguishability D as a function of the rescaled atom-cavity interaction time $\varepsilon\tau$. When $D = 1$ the which-path information is completely accessible. The parameters used are: $\lambda = 10^{-5}\text{m}$, $\varepsilon = 10^5 \text{ sec}^{-1}$, $m = 10^{-26} \text{ kg}$, $\sigma_x = \lambda/10$ and $x_0 = p_0 = 0$.

$|\langle x|\Phi_0^\pm\rangle|^2$) as functions of the rescaled atom-cavity interaction time $\varepsilon\tau$. Note how the deflection of the two outgoing paths increase as $\varepsilon\tau$ is raised up to the point that for atom-cavity interaction times larger than $\simeq 6/\varepsilon$ the two paths can be reliably distinguished through position measurements. Even fewer Rabi oscillations are needed in order for the orthogonality of $|\Phi_0^+\rangle$ and $|\Phi_0^-\rangle$ to be achieved. This is shown in Fig. 3 where the distinguishability D , according to the Englert's definition [29], is plotted as a function of $\varepsilon\tau$. In the present case, D takes the form [20]

$$D = \sqrt{\left(1 - |\langle \Phi_0^+ | \Phi_0^- \rangle|^2\right)}. \quad (30)$$

Notice how $D > 95\%$ already for $\varepsilon\tau > 1.2$. The scalar product $\langle \Phi_0^+ | \Phi_0^- \rangle$ therefore takes less time to vanish ($\simeq 1.2/\varepsilon$) than that required for distinguishing the atomic position associated with each path ($\simeq 6/\varepsilon$). The reason of such behavior is that, according to Eq. (26), the damping of $\langle \Phi_0^+ | \Phi_0^- \rangle$ is due to the trajectories in both the position and momentum space. Property (20) holds in the antinodal case as well. Indeed, using Eqs. (6), (9), (10) and (14), it turns out that, analogously to the nodal case, each scalar product $\langle \Phi_n^+ | \Phi_n^- \rangle(\tau)$ is always proportional to a damping factor. For instance, in

the case $n = 1$ it can be calculated as [22]

$$\begin{aligned} \langle \Phi_1^+(\tau) | \Phi_1^-(\tau) \rangle &= e^{i\frac{\omega_0}{2}\tau} e^{-i(a_1^2 + b_1^2)\frac{\sin(\omega_0\tau)}{\cosh(\omega_0\tau)}} \\ &\cdot e^{\frac{i}{2}\tanh(\omega_0\tau)[(a_1^2 - b_1^2)(1 + \cos(2\omega_0\tau)) + 2a_1b_1\sin(2\omega_0\tau)]} \\ &\cdot \frac{1}{\sqrt{\cosh(\omega_0\tau)}} e^{-(a_1^2 + b_1^2)(1 - \frac{\cos(\omega_0\tau)}{\cosh(\omega_0\tau)})} \\ &\cdot e^{-\tanh(\omega_0\tau)[a_1b_1(1 - \cos(2\omega_0\tau)) + \frac{1}{2}(a_1^2 - b_1^2)\sin(2\omega_0\tau)]} \\ &\propto \left[1 - \frac{(\omega_0\tau)^2}{2}\right] \cdot \exp\{-2a_1^2(\omega_0\tau)^2\} \quad (\omega_0\tau < 1) \end{aligned}$$

where $\omega_0^2 = (\hbar k^2/m\varepsilon)$, $a_1 = x_0\sqrt{m\omega_0/2\hbar}$ and $b_1 = (p_0/\sqrt{2m\hbar\omega_0})$. As in the nodal case, the damping factor is due to the increasing distance in the phase space of the deflected components of the incoming wavepacket [22].

V. CONCLUSIONS

In this paper we have presented a scheme for conditionally teleporting an unknown quantum state between two atoms interacting in succession with the same cavity mode within the optical Stern-Gerlach model. Such model, to be regarded as a generalization of the familiar Jaynes-Cummings Hamiltonian, allows to account for the atomic translational dynamics. The inclusion of such dynamics yields the well-known splitting of the wavefunction of a flying atom into a set of deflected wavepackets. Such phenomenon could be expected to have a negative effect on quantum information processing tasks. Indeed, it is known to spoil the non-local correlations between two atoms which successively interact with the same cavity mode [21, 22]. Nonetheless, in this work we have shown how exactly the above-mentioned splitting can be fruitfully exploited in order for the atomic translational degrees of freedom to behave as channels allowing efficient transmission of quantum information.

Both in the nodal and antinodal case, we have shown that successful teleportation can be obtained with probability 1/2 by measuring the number of cavity photons, the internal state of atom 2 and the position of the two atoms once they are out of the cavity. The teleportation protocol can be therefore implemented through local operations. No Bell-state measurement is thus necessary.

The essential requirement for our protocol to work is that the time of flight of each atom inside the cavity is sufficiently long in order *which-path* information to become accessible. Indeed, the initial wavepacket of each atom splits into a set of outgoing deflected wavepackets which turn out to be orthogonal, and thus distinguishable, provided the atom-cavity interaction time is large enough. Significantly, unlike previous no Bell-state measurement proposals in cavity QED, this implies a *non holonomous* constraint on the atom-cavity interaction times. No precise tuning of the atomic flight times inside the cavity is thus needed.

Nonetheless, it should be observed that, in addition, the atom-cavity interaction times must be short enough in order for the lowest-order approximation of the interaction Hamiltonian [Eqs. (3) and (4)] to hold for the whole time of flight of each atom in the cavity. However, this is not a strong constraint. Interaction times of the order of a few – say 6 – Rabi oscillations are indeed enough for a *which-path* information to be accessed (see Fig. 1). For the same reason, decoherence effects – due to the damping of the cavity mode – can be prevented [30].

Furthermore, notice that, even though the first and the second atom can be found into, respectively, two and five quantum paths, it is enough to measure only two paths for each atom (t_i^\pm associated with $|\Phi_{0,i}^\pm\rangle$) in order to teleport the initial state of atom 2 into atom 1. As emphasized in Sec. III, the labeling of such two paths is irrelevant given that it is enough to know only whether the atoms are found in the same path or not. In the latter case, the teleportation can be finalized after a 180 degree rotation around the z -axis.

Regarding the position measurements of each atom, these should be performed in such a way not to affect its internal state in the computational space $\{|g\rangle, |e\rangle\}$. This could be accomplished by sending light on the atom of wavelength suitable to excite an atomic transition different from $|g\rangle \leftrightarrow |e\rangle$.

Finally, this work opens the possibility of exploiting the atomic translational degrees of freedom in cavity QED in order to perform other typical quantum information processing tasks, such as the generation of maximally entangled states.

Acknowledgments

G. Massimo Palma (Università degli Studi di Palermo) is gratefully acknowledged for fruitful discussions and the

critical reading of the manuscript.

APPENDIX A: DERIVATION OF THE FINAL STATE

In this Appendix, we describe the procedure for obtaining the state of the system $|\Psi(t \geq t_3)\rangle$ [Eq. (16)] after that both the atoms have exited the cavity. According to Eq. (8), such state can be obtained through the successive application of operators $U_{\alpha,1}$ and $U_{\alpha,2}$ on $|\Psi(0)\rangle$ [Eq. (12)]. We first rewrite the initial state $|\Psi(0)\rangle$ [Eq. (12)] in terms of the dressed states of atom 1 by expressing $|e_1\rangle|0\rangle$ as a linear combination of $|\chi_{0,1}^+\rangle$ and $|\chi_{0,1}^-\rangle$. This yields

$$|\Psi(0)\rangle = \left(\frac{|\varphi_1(0)\rangle|\chi_{0,1}^+\rangle + |\varphi_1(0)\rangle|\chi_{0,1}^-\rangle}{\sqrt{2}} \right) |\varphi_2(0)\rangle|\alpha_2\rangle. \quad (\text{A1})$$

We now let $U_{\alpha,1}$ act on the initial state (A1) to get $|\Psi(t_1)\rangle$ (i. e. the state of the system after that atom 1 has exited the cavity). By using (15), we obtain

$$\begin{aligned} |\Psi(t_1)\rangle &= U_{\alpha,1}|\Psi(0)\rangle = \\ &= \frac{|\Phi_{0,1}^+\rangle|\chi_{0,1}^+\rangle + |\Phi_{0,1}^-\rangle|\chi_{0,1}^-\rangle}{\sqrt{2}} |\varphi_2(0)\rangle|\alpha_2\rangle. \end{aligned} \quad (\text{A2})$$

Since in the time interval between t_1 and t_2 , according to Eqs. (5) and (6), $H_\alpha^I(t) = 0$ ($\alpha = N, A$), it turns out that $|\Psi(t_2)\rangle = |\Psi(t_1)\rangle$. Before applying $U_{\alpha,2}$ to $|\Psi(t_2)\rangle$ to get $|\Psi(t_3)\rangle$, it is convenient to rearrange $|\Psi(t_2)\rangle$ as an expansion in the cavity field Fock states as

$$|\Psi(t_2)\rangle = |\Psi(t_1)\rangle = \left[\frac{|\Phi_{0,1}^+\rangle + |\Phi_{0,1}^-\rangle}{2} |e_1\rangle|0\rangle + \frac{|\Phi_{0,1}^+\rangle - |\Phi_{0,1}^-\rangle}{2} |g_1\rangle|1\rangle \right] |\varphi_2(0)\rangle \left[\cos \frac{\vartheta}{2} |e_2\rangle + e^{i\varphi} \sin \frac{\vartheta}{2} |g_2\rangle \right], \quad (\text{A3})$$

Expanding each state $|g_2\rangle|n\rangle$ and $|e_2\rangle|n\rangle$ in Eq. (A3) in terms of $|g_2\rangle|0\rangle$ and of the dressed states atom 2 $|\chi_{0,2}^\pm\rangle$ and $|\chi_{1,2}^\pm\rangle$ and, once $U_{\alpha,2}$ is applied to $|\Psi(t_2)\rangle$ with the

help of Eq. (15), the final state of Eq. (16) is obtained.

-
- [1] A. Einstein, B. Podolsky, and N. Rosen, Phys. Rev. **47**, 777 (1935).
 [2] M. A. Nielsen and I. L. Chuang, *Quantum Computation and Quantum Information* (Cambridge University Press,

- Cambridge, U. K., 2000).
 [3] C. H. Bennett, G. Brassard, C. Crpeau, R. Jozsa, A. Peres, and W. K. Wootters, Phys. Rev. Lett. **70**, 1895 (1993).

- [4] D. Bouwmeester, J.-W. Pan, K. Mattle, M. Eibl, H. Weinfurter, and A. Zeilinger, *Nature (London)* **390**, 575 (1997); D. Boschi, S. Branca, F. De Martini, L. Hardy, and S. Popescu, *Phys. Rev. Lett.* **80**, 1121 (1998).
- [5] M. A. Nielsen, E. Knill, and R. Laflamme, *Nature (London)* **396**, 52 (1998).
- [6] Q. Zhang, A. Goebel, C. Wagenknecht, Y.-A. Chen (Chen, Yu-Ao), B. Zhao, T. Yang T, A. Mair, J. Schmiedmayer, *Nat. Phys.* **2**, 678 (2006)
- [7] J. F. Sherson, H. Krauter, R. K. Olsson, B. Julsgaard, K. Hammerer, I. Cirac, E. S. Polzik, *Nature (London)* **443**, 557 (2006)
- [8] J. M. Raimond, M. Brune, and S. Haroche, *Rev. Mod. Phys.* **73**, 565 (2001).
- [9] L. Davidovich, N. Zagury, M. Brune, J. M. Raimond, and S. Haroche, *Phys. Rev. A* **50**, R895 (1994); J. I. Cirac, and A. S. Parkins, *Phys. Rev. A* **50**, R4441 (1994); S. B. Zheng and G. C. Guo, *Phys. Lett. A* **232**, 171 (1997); S. B. Zheng, *Opt. Commun.* **167**, 111 (1999); S. Bose, P. L. Knight, M. B. Plenio, and V. Vedral, *Phys. Rev. Lett.* **83**, 5158 (1999); S. Bandyopadhyay, *Phys. Rev. A* **62**, 012308 (2000).
- [10] M. Riebe, H. Häffner, C. F. Roos, W. Hänsel, J. Benhelm, G. P. T. Lancaster, T. W. Körber, C. Becher, F. Schmidt-Kaler, D. F. V. James, and R. Blatt, *Nature (London)* **429**, 734 (2004); M. D. Barrett, J. Chiaverini, T. Schaetz, J. Britton, W. M. Itano, J. D. Jost, E. Knill, C. Langer, D. Leibfried, R. Ozeri, and D. J. Wineland, *Nature (London)* **429**, 737 (2004)
- [11] L. Vaidman, *Phys. Rev. A* **49**, 1473 (1994)
- [12] N.G. de Almeida, R. Napolitano, and M. H. Y. Moussa, *Phys. Rev. A* **62**, 010101 (2000)
- [13] S.-B. Zheng, *Phys. Rev. A* **69**, 064302 (2004)
- [14] L. Ye, and G.-C. Guo, *Phys. Rev. A* **70**, 054303 (2004)
- [15] W. B. Cardoso, A. T. Avelar, B. Baseia, and N. G. de Almeida *Phys. Rev. A* **72**, 045802 (2005)
- [16] T. Sleator, T. Pfau, V. Balykin, O. Carnal, and J. Mlynek, *Phys. Rev. Lett.* **68**, 1996(1992); C. Tanguy, S. Reynaud, and C. Cohen-Tannoudji, *J. Phys. B* **17**, 4623 (1984); M. Freyberger, and A. M. Herkommer, *Phys. Rev. Lett.* **72**, 1952 (1994); A. Vaglica, *Phys. Rev. A* **54**, 3195 (1996)
- [17] R. R. Schlicher, *Opt. Comm.* **70**, 97 (1989)
- [18] M. Wilkens, Z. Bialynicka-Birula, and P. Meystre, *Phys. Rev. A* **45**, 477 (1992)
- [19] A. Vaglica, *Phys. Rev. A* **58**, 3856 (1998); I. Cusumano, A. Vaglica, and G. Vetri, *Phys. Rev. A* **66**, 043408 (2002)
- [20] M. Tumminello, A. Vaglica, and G. Vetri, *Europhys. Lett.* **65**, 785 (2004)
- [21] M. Tumminello, A. Vaglica, and G. Vetri, *Europhys. Lett.* **66**, 792 (2004)
- [22] M. Tumminello, A. Vaglica, and G. Vetri, *Eur. Phys. J. D* **36**, 235 (2005)
- [23] A. Vaglica, *Phys. Rev. A* **52**, 2319 (1995)
- [24] In the antinodal case, to be pedant, we observe that when the atomic initial wave packet is exactly centered in a field antinode and the initial momentum is 0 then the scalar products in Eq. (20) still decays exponentially but with a slower rate. Accordingly, in this case, several Rabi oscillations are necessary to neglect such scalar products in the protocol [22].
- [25] The two atoms can be always distinguished since they exit the cavity at different times.
- [26] Similarly to the seminal proposal by Bennett *et al.* [3], in such cases teleportation is finalized after a 180 degree rotation around the z -axis in the internal Hilbert space of atom 1 is performed.
- [27] M. Chianello, M. Tumminello, A. Vaglica, and G. Vetri, *Phys. Rev. A* **69**, (2004) 053403
- [28] Y. Aharonov, D.Z. Albert, and C.K. Au, *Phys. Rev. Lett.* **47**, (1981) 1029; R.F. O'Connell and A.K. Rajagopal, *Phys. Rev. Lett.* **48**, (1982) 525
- [29] B.-G. Englert, *Phys. Rev. Lett.* **77**, 2154 (1996)
- [30] S. Kuhr, S. Gleyzes, C. Guerlin, J. Bernu, U. Busk Hoff, S. Deléglise, M. Brune, J.-M. Raimond, S. Haroche, S. Osnaghi, E. Jacques, P. Bosland, and B. Visentin, *ArXiv: quant-ph/0612138*